

1 **Vegetation mapping in the St Lucia estuary using very high**
2 **resolution multispectral imagery and LiDAR**

3 *Melanie Lück-Vogel^{a, c, *}, Cikizwa Mbolambi^a, Kelly Rautenbach^b, Janine Adams^b, Lara*
4 *van Niekerk^a*

5 *^a Council for Scientific and Industrial Research, P.O. Box 320, Stellenbosch, South Africa.*

6 *^b Department of Botany, Nelson Mandela Metropolitan University, Summerstrand Campus,*
7 *6031, Port Elizabeth, South Africa.*

8 *^c Stellenbosch University, Department of Geography & Environmental Studies, 7600*
9 *Stellenbosch, South Africa.*

10 ** **Corresponding author:** E-mail address: mluckvogel@csir.co.za (M. Lück-Vogel).*

11

12 **Keywords**

13 *St Lucia, estuary, remote sensing, WorldView-2, RapidEye, SPOT-6*

14

15 **Highlights**

- 16 • High resolution satellite imagery has been assessed for estuarine habitat mapping
- 17 • All sensors, WorldView-2, RapidEye and SPOT-6 performed satisfactory
- 18 • Main causes for misclassification were wind events and estuarine water level changes

19 **Abstract**

20 This paper examines the value of very high resolution multispectral satellite imagery and

21 LiDAR derived digital elevation information for classifying estuarine vegetation types.

22 Satellite images used are from the WorldView-2, RapidEye and SPOT-6 sensors in 2m and

23 5m resolution respectively, acquired between 2010 and 2014. Ground truthing reference is a

24 GIS derived vegetation map based on field data from 2008. Supervised maximum likelihood

25 classification produced satisfactory overall accuracies between 64.3% and 77.9% for the
26 SPOT-6 and the WorldView-2 image respectively, while the RapidEye-based classifications
27 produced overall accuracies between 55.0 % and 66.8%. The reasons for the
28 misclassifications are mainly based on the highly dynamic environmental conditions causing
29 discrepancies between the field data and satellite acquisition dates rather than technical
30 issues. Dynamics in water levels and salinity caused rapid change in vegetation communities.
31 Further, weather impacts such as floods and wind events caused water turbidity and led to
32 bias in the reflective properties of the satellite images and thus misclassifications. These
33 results show, however, that the spatial and spectral resolution of modern very high resolution
34 imagery is sufficient to satisfactory map estuarine vegetation and to monitor small scale
35 change. They emphasize however the importance of synchronisation of ground truthing data
36 with actual image acquisition dates in these highly dynamic environments in order to achieve
37 high classification accuracies. The results also highlight the importance of ancillary data for
38 accurate interpretation of observed classification discrepancies and vegetation dynamics.

39

40 **1. Introduction**

41 The St Lucia Estuary is part of the uMfolozi/uMsunduzi/St Lucia estuarine system which
42 forms the largest fluvial coastal plain in South Africa (Van Heerden, 2011) and the largest
43 estuarine system in Africa (155 000 Ha). As part of the iSimangaliso Wetland Park it hosts
44 the highest biodiversity of wetland habitat types for its size in the whole of southern Africa
45 (Cowan, 1999). Besides its tremendous value for biodiversity and nature conservation, this
46 estuarine system also provides the basis for the regional economy such as commercial
47 (sugarcane) crop production, subsistence agriculture, mining, tourism, commercial and
48 subsistence forestry (GTI, 2010). While each of these activities benefits from the ecosystem

49 services of the estuarine systems, they also impact on the condition of the ecosystem in a
50 combined cumulative way.

51 The presence, abundance and condition of macrophytes, i.e. higher plants, can be used as
52 indicators to determine the health of estuarine ecosystems (EPA, 2013). However, the paucity
53 of spatial-temporal information on estuarine vegetation composition and distribution in South
54 Africa currently undermines a holistic understanding of estuarine processes and functioning
55 and subsequently the prediction of impacts of major environmental changes. Mapping of the
56 estuarine vegetation would provide a baseline for understanding and monitoring of estuarine
57 biological processes. Remote sensing is widely viewed as an effective way to spatially-
58 continuous inventories of vegetation composition, distribution and condition, in particular in
59 large and inaccessible areas in many regions of the world.

60 However, in coastal and estuarine environments, the very small scale of the habitats,
61 frequently occurring in narrow bands along the shore, prohibited the application of remote
62 sensing until recently, as most of the satellite images successfully used in other environments
63 did not provide enough spatial detail. Examples are the Landsat 4 to 8 series and the MODIS
64 and NOAA AVHRR sensors.

65 High and medium resolution data, namely aerial photographs, SPOT 3 and Landsat TM
66 imagery have been compared by Harvey and Hill (2001) in the Northern Territory, Australia,
67 to determine the accuracy and applicability of each data source for the detailed spectral
68 discrimination of vegetation types in a tropical wetland. They found that aerial photos with a
69 very high spatial resolution provided better classification accuracies than the SPOT and
70 Landsat TM imagery. In accordance with this, Yang (2007) classified riparian vegetation in
71 Australia with an accuracy of 81% using aerial photos, 63% using SPOT-4 imagery (10m
72 resolution) and 53% using Landsat 7 imagery (30m resolution). He pointed out that the low

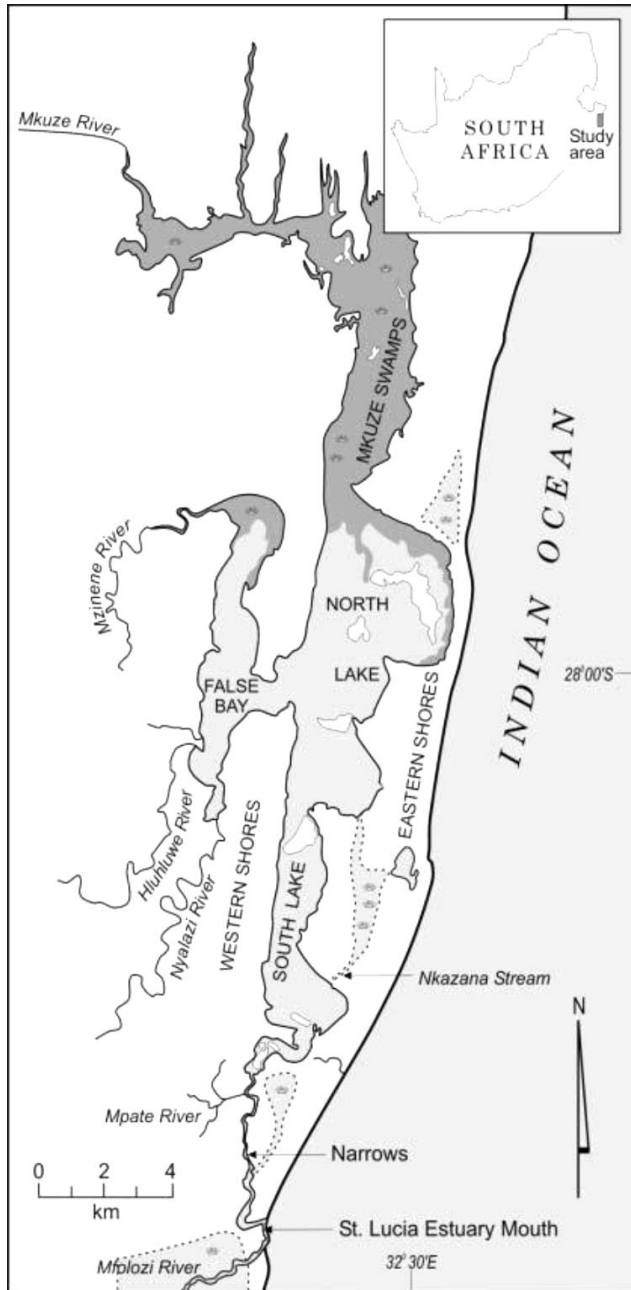
73 number of spectral bands is the limiting factor in using aerial photos for wetland vegetation
74 classification, as is the coarse spatial resolution in the case of the Landsat imagery.
75 Only with the recent availability of very high resolution (VHR) imagery e.g. from the SPOT-
76 6, RapidEye and Worldview-2 sensors which provide multispectral imagery with pixel sizes
77 between 2 and 5 meters and more spectral bands, satellite remote sensing of estuarine and
78 coastal regions has become more feasible. In addition, topographic information derived from
79 airborne LiDAR (Light Detection and Ranging) technology has proven to improve coastal
80 vegetation mapping significantly, in particular when used in combination with multispectral
81 imagery (Prisloe et al., 2006; Kempeneers et al., 2009).
82 The aim of this paper was therefore to test and compare the use of VHR SPOT-6, RapidEye
83 and WorldView-2 (WV2) satellite imagery with and without combination of LiDAR data for
84 mapping relevant vegetation types in the St Lucia Estuary.
85 The classes that were mapped were aligned with existing habitat keys from the National
86 Biodiversity Assessment (Van Niekerk and Turpie, 2012; Turpie et al., 2012). The intention
87 was to provide guidance on which sensor or sensor combination provides the most accurate
88 spatial information for informing estuarine management. Furthermore, the influence of
89 environmental factors such as wind speed and water levels on the accuracy of the results was
90 examined.

91

92 **2. Study area**

93 With an area of about 30 520 ha, St Lucia is the largest estuary in South Africa (Moll et al.
94 1971; Turpie et al. 2012). The climate is subtropical with an average annual rainfall of
95 approximately 1100 mm with most rainfall occurring in winter and spring i.e. June to October
96 (Taylor et al., 2006). The average temperatures range between 25-28°C throughout the year.

97 In the south the estuary mouth is connected to the Indian Ocean by the 21 km long Narrows
98 channel. The lake system is separated from the sea by high coastal dunes that flank its eastern
99 bank (Taylor, 2006).



100

101 **Figure 1: The St Lucia system including its lakes and feeder rivers (Source: Whitfield**
102 **1992).**

103

104 St Lucia has an inlet/mouth that is periodically closed to the sea for months to years at a time
105 depending on the river inflow regime and management interventions. This means that water

106 levels and salinity can change drastically within short periods, e.g. after floods and mouth
 107 breaks. In response, the distribution of estuarine vegetation communities is highly dynamic.
 108 The predominant natural estuarine vegetation in the region can be divided into 8 habitat units,
 109 namely permanently flooded macroalgae and submerged macrophytes, partly flooded reeds
 110 and sedges and salt marshes, mangroves and swamp forests, and grass and shrub vegetation,
 111 and lastly floating macrophytes (Rautenbach, 2015). Table 1 below summarises the dominant
 112 species and gives a brief description of these habitat types.

113 **Table 1: Habitat units and their dominant species (Rautenbach, 2015).**

Habitat Unit	Dominant Species	Description
Macroalgae	<i>Ulva intestinalis</i> , <i>Chaetomorpha</i> sp., <i>Cladophora</i> sp., <i>Bostrychia</i> sp. and <i>Polysiphonia</i> sp.	Found at estuary margins, as epiphytes and associated with mangrove pneumatophores.
Submerged macrophytes	<i>Ruppia cirrhosa</i> , <i>Zostera capensis</i> and <i>Stuckenia pectinata</i>	Plants rooted in substrata whose leaves and stems are completely submersed.
Reeds and sedges	<i>Phragmites australis</i> , <i>Juncus kraussii</i> and <i>Schoenoplectus scirpoides</i>	Observed at sites with freshwater input at the margins, rooted in submerged substrata. <i>Juncus kraussii</i> is observed at the vicinity of the Forks and the Narrows.
Mangroves	<i>Avicennia marina</i> and <i>Bruguiera gymnorhiza</i>	Observed in the brackish to saline intertidal areas at the Narrows and mouth area.
Grass and shrubs	<i>Sporobolus virginicus</i> , <i>Paspalum vaginatum</i> and <i>Stenotaphrum secundatum</i>	Sedge grass and shore slope lawn, observed in areas where there is no freshwater input, freshwater is provided by rainfall.
Salt marsh	<i>Sarcocornia</i> sp., <i>Salicornia meyeriana</i> and <i>Atriplex patula</i>	Succulent species colonize exposed saline soils in False Bay and in the mudflats of North Lake and are not tolerant to long periods of inundation.
Swamp forest	<i>Ficus trichopoda</i> , <i>Barringtonia racemosa</i> and <i>Voacanga</i> sp.	Observed on the banks of Mfolozi Estuary, in the vicinity of the back channel and Narrows and along the Eastern Shores under freshwater conditions.
Floating macrophytes	<i>Nymphaea nouchal</i> , <i>Azolla filiculoides</i>	Floating leaved species are commonly associated with submerged and deepwater aquatics and occur at water depths from 0.5 to 2 m.

114
115
116
117
118
119
120
121
122
123
124
125
126
127
128
129
130
131
132
133
134
135
136
137
138

Land use in the vicinity of the estuarine system is diverse. It includes commercial (sugarcane) crop production, subsistence agriculture, mining, tourism, commercial and subsistence forestry, conservation as well as residential areas (GTI, 2010). The land use in the immediate iSimangaliso Wetland Park (former Greater St Lucia Wetland Park) area changed dramatically during the last two decades. Before the declaration of the Wetland Park as UNESCO World Heritage Site in 1999 (UNESCO, 1999), large areas were used for commercial forestry, introducing alien Eucalypt and Pine species. Since the foundation of the Wetland Park, forestry has been actively removed, and international eco-tourism is becoming more important. In the abandoned forestry areas, a quick succession of natural vegetation can be observed. However, an expansion of rural settlements into the area due to an increase in population (e.g. immigration from Mozambique and other areas), puts a new pressure on natural environments.

3. Material and methods

3.1. Input data

3.1.1. Reference habitat map

As reference map for this study an existing GIS map based on aerial imagery from 2008 was used. The map only delineates habitats below the 5m contour. This map was originally generated by Nondoda (2012). A modified version of this map as presented by Rautenbach (2015) which aggregates some of Nondoda's original classes was used for this study. Accuracy and spatial detail was considered suitable for our purpose. The habitat units derived from this data set are Submerged macrophytes, Salt marsh, Swamp forest, Grass and shrubs, mangroves, and Reeds & Sedges (see Table 1 above).

139 **3.1.2. LiDAR data**

140 A LiDAR data set acquired in April-May 2013 covering the iSimangaliso Wetland Park area
141 was made available for this project by the iSimangaliso Wetland Park authority. The Digital
142 Terrain Model (DTM) data consisted of high accuracy (1 Sigma) point data of LiDAR
143 derived surface information, which has been provided in xyz ASCII format as well as in
144 0.25m contours in SHP file format. The ASCII format contains very detailed surface
145 information. However, files tend to be huge and require special software to access. In
146 contrast, the SHP format is a format that most GIS practitioners can readily use and it is
147 therefore a common LiDAR output product format. However, the generalisation of the
148 information to derive 25cm contours means a loss of detail. In order to assess the impact of
149 this loss of detail on the habitat classification accuracy, in this project both the SHP file
150 contour product and the raw, unthinned xyz point cloud data binned to 1 meter were used as
151 separate inputs for the habitat classification.

152

153 **3.1.3. Satellite imagery**

154 For this project, a series of high resolution satellite images from the RapidEye, SPOT-6 and
155 WorldView-2 sensors was acquired. All imagery was provided in full band mode,
156 geometrically but not radiometrically corrected (level 2B). Table 2 below gives an overview
157 of the respective sensors, the spatial resolution and the respective acquisition dates. The
158 respective spectral bands are given in Table 3 below.

159

160

Table 2: Satellite data used and their specifications

Sensor	Resolution (m)	Acquisition Dates
WorldView-2	2.0	9 April 2010
RapidEye	5.0	18/20 July 2011

		13 January 2012
SPOT6	5.0	8 February 2014
LiDAR	Rasterised to match above	April-May 2013

161

162 **3.2. Areas used for application of approach**

163 For the supervised classification approach only subsets of the total satellite coverage were
 164 used which corresponded largely with the extent of the Wetland Park and the extent of the
 165 reference habitat map. In this way, land cover and habitat classes for which no reference data
 166 were available and whose accuracy could not have been assessed (e.g. any agriculture and
 167 other transformed areas) were largely excluded. The available RapidEye and SPOT-6 data
 168 covered almost the full extent of that area, while for WorldView-2 only for the southern part
 169 imagery was available.

170

171 **3.3. Methods**

172 The final goal of comparing habitat classifications derived from different combinations of
 173 input data has been achieved following several pre-processing, data conversion and data
 174 generation steps. Figure 2 gives an overview of the work conducted for the Maximum
 175 Likelihood classification. The individual pre-processing, classification and post-processing
 176 steps are unpacked in the following sections.

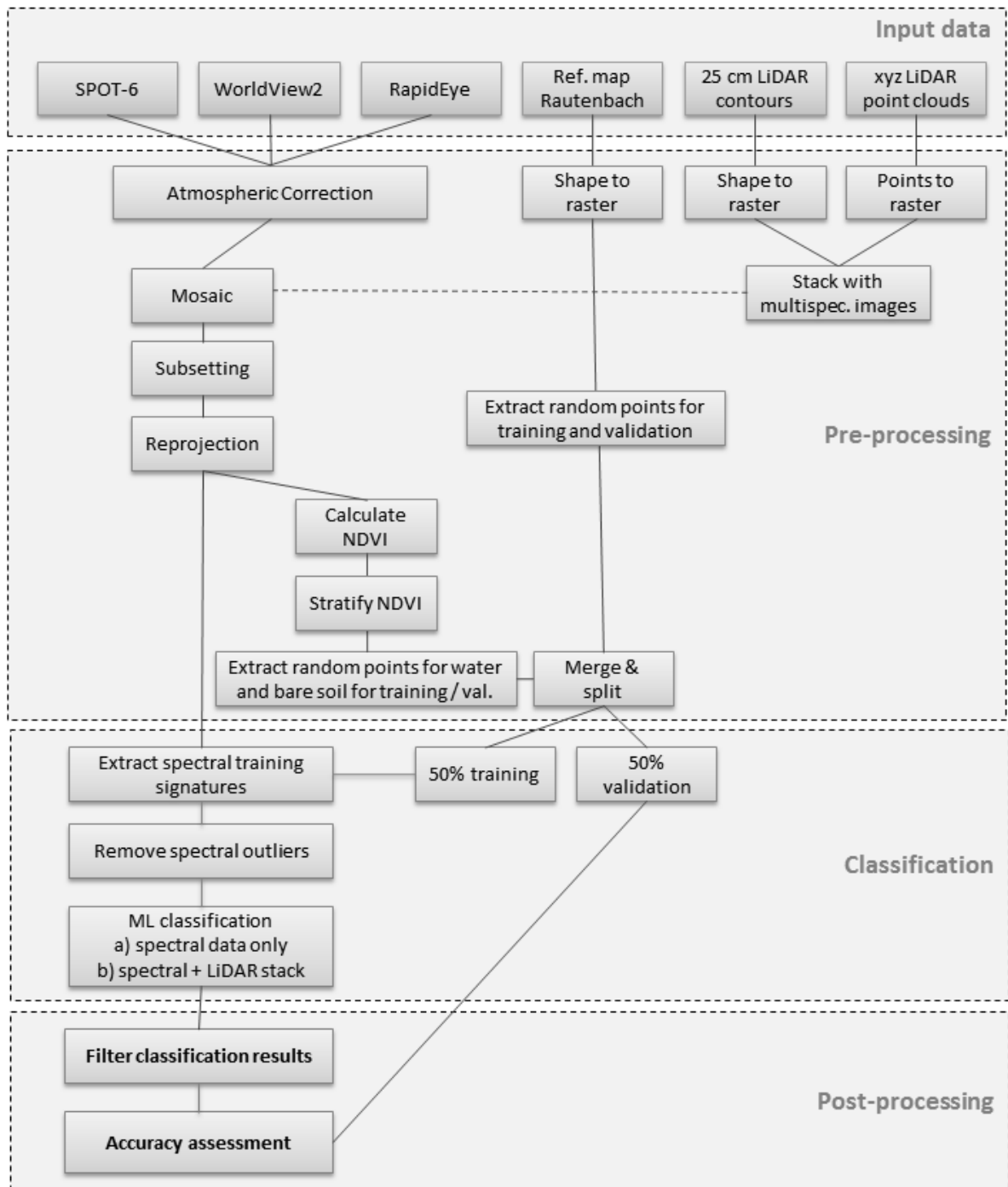


Figure 2: Flow diagram of technical steps conducted.

177

178

179

3.3.1. Preprocessing of remote sensing data

180

All satellite image files were corrected for radiometric and atmospheric effects to derive top

181

of canopy reflectance values. This correction allowed for better analysis of the spectral

182

signatures in the actual classification approach as described in Section 3.3.4 below.

183 The RapidEye image for July 2011 was provided as seven individual tiles from two separate
184 acquisition dates (18 and 20 July 2011), the RapidEye image for 13 January 2012 as six
185 individual tiles. Following the atmospheric correction of the individual tiles, all the tiles for
186 July 2011 and all tiles for January 2012 were mosaicked to allow for an easier handling of the
187 data in the subsequent work steps.

188 Some of the satellite images originally came in UTM projection with WGS84 Datum, while
189 others were provided in Transverse Mercator projection. It was decided to reproject all
190 images to the projection of the 2008 reference data: Transverse Mercator, Central Meridian
191 33°E, Hartebeesthoek 1994 Datum. In this way, the best possible geographical match of the
192 data sets was achieved. It is important that the images to be classified overlay with high
193 geographic accuracy to the reference data, as spatial misalignments can lead to
194 misclassifications and reduced accuracies (Townshend et al. 1992).

195 Given the humid, subtropical climate of the area, it was very difficult to get 100% cloud free
196 satellite images; three out of the four images used had some cloud occurrences. A masking of
197 cloud areas was not conducted as a result of time constraints. However, in order to avoid
198 biases in the classification and accuracy results, care was taken in the selection of cloud-free
199 training and validation points instead (Section 3.3.2 and 3.3.3).

200 The LiDAR data for that area were provided in individual small tiles as well. Therefore, in a
201 first step, those tiles covering the SPOT-6, RapidEye and WV-2 mosaics were identified.

202 For those, both, the 25cm contour SHP files as well as the unthinned xyz ASCII files binned
203 to 1m resolution were converted into an ERDAS IMG raster format matching the spatial
204 resolution of the respective multispectral images (2m and 5m respectively). The raster tiles
205 were then mosaicked and reprojected to match the projection of the multispectral mosaics.
206 The elevation data ranges were then stretched and the layers were stacked (i.e. attached) to
207 the respective multispectral images (see respective last layers “contour DEM” and “xyz

DEM” in Table 3 below). The elevation range of the original Terrain model for that area was between -2.5 m to + 180 m. This data range is very small when compared to the re-scaled reflectance values of the multispectral images, ranging typically between 500 and 6000. The original small data range of the elevation data would be almost un-noticeable when attached as extra layer to the multispectral image, thus not adding much information for the Maximum Likelihood classification. Therefore the DEM data were re-scaled using the function $[(Image + 2.5) * 100]$, leading to a “stretched” data range between 0 and 18250 which emphasises small variations in relief. Altogether 8 data stacks were produced as input for the classification process (Table 3).

Table 3: Bands of the respective layer stacks used for the supervised classification process.

Stack No.	1	2	3	4	5	6	7	8
Band No	WV-2	WV-2	RapidEye 2011	RapidEye 2011	RapidEye 2012	RapidEye 2012	SPOT-6	SPOT-6
1	Coastal	Coastal	Blue	Blue	Blue	Blue	Blue	Blue
2	Blue	Blue	Green	Green	Green	Green	Green	Green
3	Green	Green	Red	Red	Red	Red	Red	Red
4	Yellow	Yellow	RedEdge	RedEdge	RedEdge	RedEdge	NIR	NIR
5	Red	Red	NIR	NIR	NIR	NIR	Contour DEM	xyz DEM
6	RedEdge	RedEdge	Contour DEM	xyz DEM	Contour DEM	xyz DEM		
7	NIR1	NIR1						
8	NIR2	NIR2						
9	Contour DEM	xyz DEM						

217

218

219 **3.3.2. Extraction of ground truthing points from GIS reference data**

220 Basis for the training and validation data for the classification of the satellite images was the
221 2008 reference map (Section 3.1.1). For the classes Submerged macrophytes, Salt marsh,
222 Swamp forest, Grass and shrubs, Mangroves and Reeds & sedges (Table 1) stratified random
223 points were extracted from that map (Duro et al., 2012; Lowry et al., 2007). Between 20 and
224 30 points per class per satellite image extent were created. For all resulting points it was
225 checked visually if any of them was lying in an area impacted by clouds or cloud shadows.
226 Impacted points were omitted to avoid biases in the classification and validation approach.

227 **3.3.3. Extraction of ground truthing points for bare soil and open water**

229 Additional random points for the land cover classes Open water and Bare soil were created,
230 as these classes are highly important in an estuarine and coastal context and it was anticipated
231 that the inclusion of training points for these classes would improve the overall accuracy of
232 the supervised maximum likelihood classification in narrowing the actual feature space for all
233 classes.

234 For the identification of open water and bare soil area, the normalised Difference Vegetation
235 Index (NDVI) was calculated for all four images, following the formula $NDVI = (NIR - Red) / (NIR + Red)$.
236 The value range for NDVI data is from -1 to +1. It is generally accepted that
237 NDVI values for open water are lower than 0, and values for bare soil are in the positive
238 range just above 0 if images are derived from radiometrically corrected images, as in our case
239 (Loveland et al., 1991; Lunetta et al., 2006). Visual inspection of the actual NDVI data
240 confirmed this rule, only for the RapidEye-derived NDVI data the threshold between water
241 and bare soil had to be adjusted to 0.1 for a visually satisfactory distinction between the two
242 classes.

243 For Bare soil, an NDVI value range between 0.0 (0.1 for RapidEye) and 0.4 was set. The
244 threshold of 0.4 for delineating bare soil from vegetation appears to be quite high. However,

245 impervious surfaces (i.e. anthropogenic bare surfaces) were characterised by Loveland et al.
246 (1991) by values between 0.3 and 0.4, too. However, for this paper, the threshold has been
247 defined visually from the image, using fallow fields, roads and the beach as reference. It
248 cannot be excluded though that our class “Bare Soil” would include some sparse vegetation,
249 too.

250 From the derived Water and Bare Soil masks about 25 random points were extracted for both,
251 training and validation and added to the respective point sets created from the 2008 habitat
252 reference map. Points impacted by clouds and cloud shadows were removed from these
253 classes as well. For the resulting eight habitat classes, between 154 (WV-2) and 251
254 (RapidEye) training and validation points respectively were used. The variation in point
255 numbers is related to the amount of points which had to be deleted due to cloud and cloud
256 shadow impact. Further, in the 2008 reference map Salt marsh and Submerged macrophytes
257 did not occur in the southern area covered by the WV-2 image, thus these classes are not
258 represented in the WV-2 classification.

259

260 **3.3.4. Maximum Likelihood classification**

261 For all four images spectral training signatures were created for the respective training points
262 for all eight respective layer stacks (Table 3). The resulting spectral signatures were cleaned
263 from obvious outliers that would have contributed to biased spectral statistics in the following
264 classification process. Outliers were caused mainly by changes in land cover in the time
265 between the 2008 reference data and the actual image acquisition date, such as forest
266 plantation to grass and shrubs, or grass and shrubs to swamp forest. Where the analysis of the
267 spectral signatures revealed that there are spectral subgroupings within one of the reference
268 classes, these subclasses were treated as individual classes during the classification process.
269 As an example, the class “Grasses and Shrubs” consisted of areas which were clearly

270 dominated by shrubs, while other areas were dominated by grasses, resulting in either more
271 shrub or grass dominated spectral signatures. Here subclasses “Grass and shrubs_woody” and
272 Grass and shrubs_grassy” were created. Furthermore some of the reeds were flooded during
273 the time of image acquisition and looked spectrally different from non-flooded reeds.
274 Keeping these spectrally different subgroups of a class separate in the actual classification
275 process has shown to produce higher classification accuracies. The classification process was
276 then run on all 8 layer stacks (as per Table 3) twice, first excluding, then including the
277 contour and xyz DEM respectively, resulting in a total of 16 classifications.

278

279 It was decided to include all multispectral bands of the respective sensors in the classification
280 process to assess the value of the high spectral resolution (i.e. increased number of bands) on
281 the accuracy of the classification results. Schuster et al. (2012) and Adam et al. (2014)
282 emphasise the improvement of land cover classifications by using RapidEye’s RedEdge band.
283 For all classifications, Feature Space was selected as the non-parametric rule and Maximum
284 Likelihood as the parametric rule in ERDAS’ Supervised classification tool.

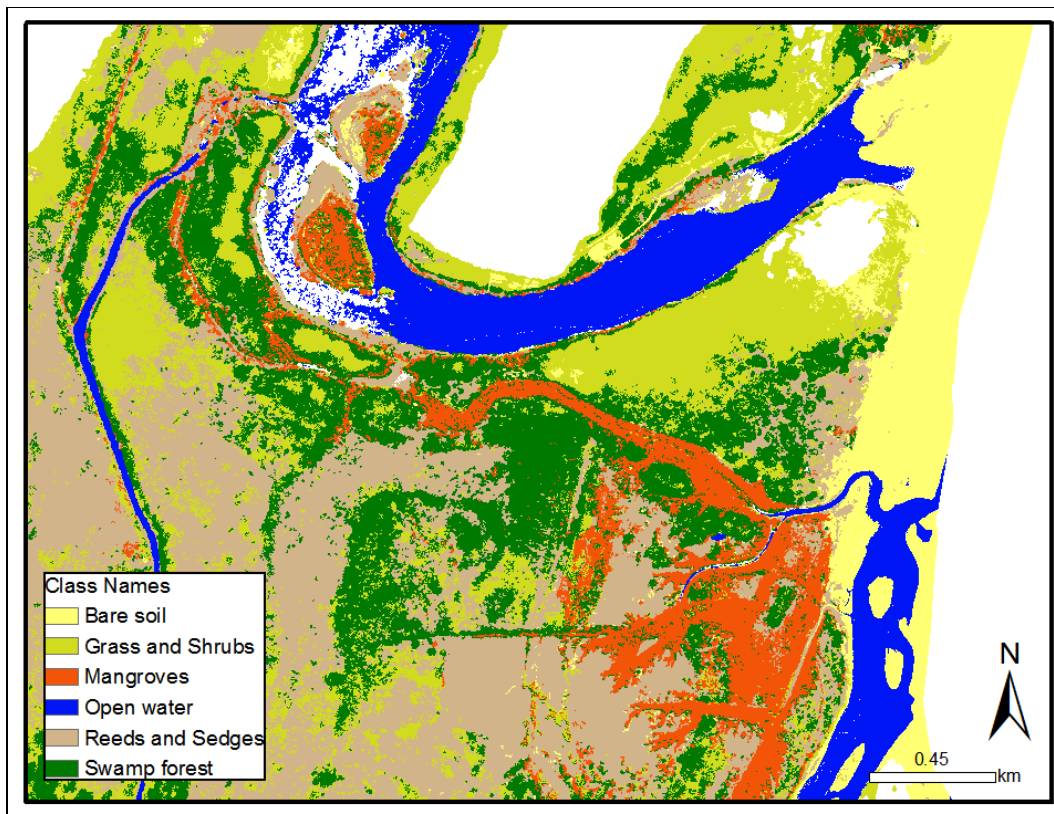
285

286 **3.3.5. Post-Processing**

287 Given the high spatial resolution of the satellite images, the 16 classification results looked
288 very “noisy”. This means that the vegetation types were disrupted by single classes or groups
289 of pixels of another class, mainly as a result of shadow effects in the vegetation canopy. It
290 was therefore decided to filter the classification outputs to eliminate those miss-classified
291 single pixels or small pixel groups consisting of <8 pixels (Figure 3). According to Duro et
292 al. (2012) this smoothing of classification results can improve the overall classification
293 accuracy.

294 Further, where existing, the interim subclasses (e.g. Sedges and Reeds-flooded and Sedges
295 and Reeds-non-flooded) were merged again to the original class types. This had to be done to
296 have the same level of class detail as the reference habitat map for accuracy assessment
297 purposes.





298 **Figure 3: Example of classification results. Top: Multispectral WV-2 image of the**
 299 **estuary mouth; Bottom: final classification results for same area after filtering (areas**
 300 **higher than 10m above sea level are masked out).**
 301

3.3.6. Accuracy Assessment

302
 303 For all resulting 16 classifications, error matrices including the Overall Accuracy, the User's
 304 and Producer's Accuracy for each class as well as the Kappa coefficient were produced and
 305 analysed. The Overall Accuracy gives the percentage of reference points that have been
 306 classified correctly. The User's Accuracy indicates the probability that a pixel classified in
 307 this class actually represents this class on the ground, and the Producer's Accuracy indicates
 308 how accurately the training points have been classified. The Kappa statistic indicates to
 309 which extent the classification result is better than pure chance (Lillesand et al. 2004), i.e. the
 310 higher the Kappa value, the greater the classification accuracy. The difference between
 311 Kappa and Overall Accuracy (OAA) is that the OAA can be biased by differences in the

312 number of reference points per class, i.e. classes with more reference points weigh more in
 313 the OAA, while the Kappa is not affected by unequal reference point numbers.

314

315 **4. Results and Discussion**

316 Table 4 below gives an overview of the Overall Accuracies and Kappa values for all 16 (4 x
 317 4) classification runs.

318

319 **Table 4: Overview of overall accuracies (OAA) and Kappa values for all classifications.**

320

Run no.	DEM type	2010 WV-2		2011 RapidEye		2012 RapidEye		2014 SPOT-6	
		OAA	Kappa	OAA	Kappa	OAA	Kappa	OAA	Kappa
1	no contours	72.7%	0.66	57.8%	0.52	55.0%	0.48	69.6%	0.64
2	contours	76.6%	0.70	62.5%	0.57	60.2%	0.54	64.3%	0.59
3	no xyz	75.3%	0.69	57.4%	0.51	56.8%	0.50	71.4%	0.67
4	with xyz	77.9%	0.72	66.8%	0.62	57.8%	0.51	75.7%	0.72

321

322

323 **4.1. Impact of LiDAR DEMs on classification accuracies**

324 Comparing runs 1 and 2, and runs 3 and 4 in Table 4 respectively shows that in 7 out of the 8
 325 classifications the additional use of the LiDAR derived DEM information improved the
 326 overall classification accuracies (OAA). This result is in accordance to other publications,
 327 confirming that the combined use of LiDAR and multispectral data improves classification
 328 accuracies (e.g. Kempeneers et al. 2009). The LiDAR decreased the accuracy of the
 329 classification results in the second run of the SPOT-6 image.

330 The overall accuracies and Kappas for the purely multispectral based classifications of the
 331 first and third run are about the same for the RapidEye and SPOT-6 images, which was to be
 332 expected because in both cases the input is only the multispectral image. However, there is a

333 slight improvement in the third run of the WorldView-2 image, probably caused by slight
 334 differences in the respective training areas.
 335 Accuracies for three of the four classifications including the detailed LiDAR information in
 336 the fourth run are higher than the respective accuracies for the contour-derived LiDAR stacks
 337 in run 2. This indicates that the use of more detailed surface data improves vegetation
 338 classification accuracies.

339

340 **4.2. Confusion between Sedges & Reeds and Grass & Shrubs**

341 Table 5 shows the error matrix for the fourth run of the WorldView-2 classification that
 342 included the detailed xyz-derived LiDAR data. This matrix shows how many of the reference
 343 data have been classified correctly. For example, of the 19 validation points for Grass and
 344 Shrubs (row Ref. Total), 13 have been correctly classified as Grass and Shrubs, but 2 points
 345 were classified as Swamp forest and Sedges and Reeds and one as Mangroves and one as
 346 Bare soil. Altogether, 33 points have been classified as Grass and Shrubs (Class. Total), 13 of
 347 which are in fact Grass and Shrubs, but 9 of the 33 should have been classified as Swamp
 348 forest, 1 as Mangroves and 10 as Sedges and Reeds instead. The last columns give the
 349 respective Producer's and User's Accuracy and Kappa value per class.

350 **Table 5: Error matrix for the 4th run of the WorldView-2 classification of the stack**
 351 **including the xyz-derived LiDAR information.**

Classified Data	Sw. forest	G & S	Mangr.	Open water	Bare soil	S & R	Class. Total	Prod. Acc.	Users Acc.	Kappa
Sw. forest	45	2	1	0	0	0	48	81.8%	93.8%	0.90
Gr. & Shrub	9	13	1	0	0	10	33	68.4%	39.4%	0.31
Mangroves	1	1	7	0	0	0	9	70.0%	77.8%	0.76
Open water	0	0	0	22	0	0	22	81.5%	100%	1.00
Bare soil	0	1	1	3	14	0	19	100%	73.7%	0.71
S. & Reeds	0	2	0	0	0	19	21	65.5%	90.5%	0.88
Ref. Total	55	19	10	25	14	29	152			

Overall Classification Accuracy = 77.92%

Overall Kappa Statistics = 0.723

352

353 Table 5 shows that the accuracies for 5 of the 6 classes with Kappas >0.7 are quite high,
354 including the classes Bare soil and Water, which, because of their spectral distinctness from
355 any vegetation classes, in most land cover classifications yield very high accuracies.
356 However, the sensors often confused the classes Grass & Shrubs and Sedges & Reeds,
357 leading to Kappas as low as 0.31 and Accuracies as low as 39.4%. The analysis of the other
358 classifications shows that the same confusion occurred frequently between these two classes.
359 However, we expect that the high dynamic of the estuarine vegetation, in particular the non-
360 woody classes even over a relatively short observation period of two years would be the main
361 reason for the low accuracy results when measured against the 2008 reference data. High
362 dynamics in the estuarine vegetation have also been reported by Rautenbach (2015) for the
363 period 2008-2013. In other words, our classifications correctly picked up real vegetation
364 changes on the ground.

365 Further sources for low classification accuracies are:

- 366 - **Spectral similarity between the classes:** The more grassy areas of the class Grass and
367 Shrubs might have gotten confused with the also grass-like Sedges & Reeds.
- 368 - **Small scale vegetation mosaic:** In case that the vegetation on the ground appears in
369 form of a mosaic of small patches of different vegetation types and that this patchiness
370 had been “generalised” in the 2008 reference map, this might confuse the classification
371 in that either the classifier picked variations up correctly but the generalised reference
372 data did not have the correct resolution, or in the form of spectral mixed pixels, which
373 are “blurry” and do not pick up boundaries between patches correctly.
- 374 - **Different water levels:** both vegetation types are bound to sites which are low lying and
375 prone to (and dependent on) various levels of flooding. So even if the vegetation itself
376 did not change between the image date and the reference date, various levels of flooding,
377 spatially and temporally, might have biased the spectral signatures and lead to confusion

378 between these classes. This observation is confirmed by the findings of Fyfe (2003) and
379 Silva et al. (2008) whose wetland classifications were affected by similar effects. Figure
380 5 and Figure 6 also illustrate the varying water levels in the area at the time of the
381 satellite observations.

382 - **Accuracy of the reference data:** The St Lucia wetlands cover a large area and under
383 various water levels all sections are not equally accessible (e.g. swampy area with large
384 populations of hippopotami and crocodiles). It stands to reason that in the 2008 reference
385 map some areas were therefore mapped at a coarser resolution than others. It can
386 therefore not be excluded that those two classes have been confused in that data already.

387

388 **4.3. Analysis of accuracies of other classes**

389 Figure 4 below shows the Kappa values for all 8 classes in all 16 classifications. The figure
390 shows that the accuracy for class Submerged macrophytes is consistently high for all three
391 images (class not present in smaller WorldView-2 image extent). This result is in contrast to
392 other findings, e.g. by Adam et al. (2009) who found that submerged vegetation is difficult to
393 distinguish due to the high water fraction in the spectral signal. Reflectance of water in the
394 Infrared band is close to zero, while vegetation has high reflectance in Infrared and
395 distinction between species frequently relies on these bands. However, Dogan et al. (2009)
396 used Quickbird data for successful mapping of submerged vegetation as well which provides
397 4 spectral bands (visible plus near infrared) in 0.65 m resolution.

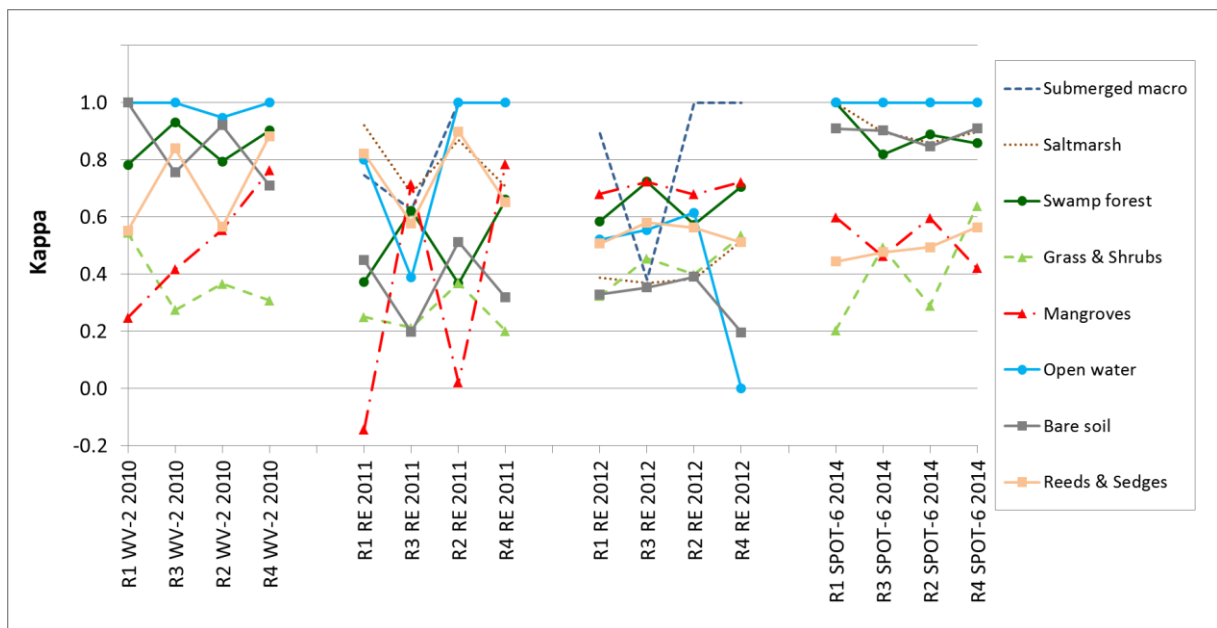
398 Similarly, Swamp forest was consistently mapped with very high accuracies, apart from the
399 DEM-including runs 2 and 4 of the RapidEye images. In contrast, the class Grass and Shrubs
400 frequently was amongst the lowest accuracies. Mangroves have been classified satisfactory in
401 most of the classifications, too; only in run 1 and run 2 of the 2011 RapidEye image they got

402 confused with Swamp Forest, which means, here the additional use of the DEM increased the
 403 separability between the two forest types.

404 The class Open Water was amongst the best classes in most of the images, which was
 405 expected. Water and Bare soil were classified with very low accuracies however in the
 406 RapidEye images, and the reasons for this are discussed in section 4.5 below.

407 The implication of these results for the user is that Submerged macrophytes, Swamp forest,
 408 Mangroves, Open water and Bare soil are those classes which – according to our results – can
 409 be extracted most reliably from the compared WorldView-2, RapidEye and SPOT-6 images,
 410 while the other classes, in particular those with continuously low accuracies are not so easily
 411 distinguishable in an approach as the presented one.

412



413

414 **Figure 4: Kappa values for all classes in all 16 classification runs. R1 and R3: runs**
 415 **without LiDAR DEM, run R2: with contour DEM, run R4: with xyz DEM.**

416

417 **4.4. Comparison of accuracies between sensors**

418 Generally, WorldView-2 produced the best accuracies and SPOT-6 the second best results,
 419 while all the RapidEye classifications have strikingly low accuracies (Table 4) with overall

420 accuracies between 55.0 and 66.8% and Kappas as low as 0.48 to 0.62. The good WV-2
421 result is expected, given the closest temporal “proximity” to the 2008 reference data. It might
422 be premature though to conclude that WorldView-2 also having the highest spectral and
423 spatial resolution (8 bands, 2m pixel size) of the compared data sets is the most appropriate
424 for estuarine habitat classification, as, given to the smaller extent of the available image, the
425 total number of classes was lower than in the other images as Submerged macrophytes and
426 Salt marsh did not occur in that area. A lower number of classes usually increases
427 classification accuracies.

428 SPOT-6 has only 4 spectral bands and a pixel size of 5 meters, and with its 10 vegetation
429 classes it still produced the second best results, which is even more striking, given its largest
430 temporal “distance” from the 2008 reference data. In contrast, both RapidEye images with 5
431 spectral bands and also 5 meter pixel size produced unsatisfactory accuracies for many
432 classes. In comparison, Adam et al. (2014) achieved accuracies above 90% for their
433 RapidEye based land cover classification in the same region. However, their classes were
434 much broader (bare land, coastal sand, grassland, degraded grassland, indigenous forest,
435 mature sugarcane, young sugarcane, plantation forest, settlements, water body and wetland)
436 and spectrally more distinct and thus less prone to misclassification than the classes used in
437 this study, where Adam’s class “Wetland” actually is divided into six subclasses.

438
439 Given the inconsistency of accuracies for individual classes between the compared sensors, in
440 this study the results are not used for a change analysis of over time, as the results are likely
441 biased by the respective class-related errors.

442

443 **4.5. Analysis of 2011 and 2012 RapidEye results using environmental condition data**

444 Table 6 shows the error matrix for the 2011 RapidEye classification of the stack including the
 445 xyz-derived LiDAR information (run 4) as a typical example for the RapidEye results. Table
 446 7 shows the accuracy matrix for the fourth run of the 2012 RapidEye classification.

447 **Table 6: Error matrix for the 2011 RapidEye classification of the stack including the**
 448 **xyz-derived LiDAR information.**

Classified Data	Subm.	Salt marsh	Swamp forest	G & S	Mangr.	Open water	Bare soil	S & R	Ref. Totals	Prod. Acc.	Users Acc.	Kappa
Submerged	20	0	0	0	0	0	0	0	23	87.0%	100.0%	1.00
Salt marsh	0	20	0	4	0	1	0	2	24	83.3%	74.1%	0.71
Sw. forest	0	0	22	5	1	0	0	3	29	75.9%	71.0%	0.66
Gr. & Shrub	0	2	0	7	3	0	7	6	20	35.0%	28.0%	0.20
Mangroves	0	0	3	0	17	0	0	1	23	73.9%	81.0%	0.79
Open water	0	0	0	0	0	9	0	0	23	39.1%	100.0%	1.00
Bare soil	3	1	0	0	0	13	11	1	18	61.1%	37.9%	0.32
S. & Reeds	0	1	4	4	2	0	0	29	42	69.1%	72.5%	0.65
Col.Total	23	24	29	20	23	23	18	42	202			

Overall Classification Accuracy = 66.83%

Overall Kappa Statistics = 0.62

450
 451 In the 2011 result, the class Sedges and Reeds for the reasons described above is confused
 452 with Grass and Shrubs. However, in this image, Grass and Shrubs also was confused with
 453 Bare soil. It has to be remembered though, that the Bare Soil mask was produced using an
 454 NDVI threshold of 0.4, which is likely to include sparsely vegetated areas as well (compare
 455 section 3.3.3). It is therefore possible that some open Grass and Shrub areas, maybe areas
 456 recovering after vegetation removal, wrongly fell into the Bare soil class. Further, probably
 457 the more woody fraction of the Grass and Shrubs class got confused to a greater extent with
 458 the other woody class Swamp forest. Apparently RapidEye’s spectral resolution was not good
 459 enough to distinguish between these spectrally similar classes.

461 **Table 7: Error matrix for the 2012 RapidEye classification of the stack including the**
 462 **xyz-derived DEM information.**

Classified Data	Subm.	Salt marsh	Swamp forest	G & S	Mangr.	Open water	Bare soil	S & R	Ref. Totals	Prod. Acc.	Users Acc.	Kappa
Submerged	13	0	0	0	0	0	0	0	18	72.2%	100.0%	1.00
Salt marsh	0	8	0	3	2	0	0	1	26	30.8%	57.1%	0.52
Sw. forest	0	0	26	3	4	0	0	2	29	89.7%	74.3%	0.71
Gr. & Shrub	0	5	1	24	3	0	3	3	40	60.0%	61.5%	0.53
Mangroves	0	0	0	0	12	0	0	4	23	52.2%	75.0%	0.72
Open water	0	0	0	0	0	0	0	0	25	---	---	0.00
Bare soil	5	8	0	2	0	25	16	1	24	66.7%	28.1%	0.20
S. & Reeds	0	5	2	8	2	0	5	34	45	75.6%	60.7%	0.51
Col. Total	18	26	29	40	23	25	24	45	230			

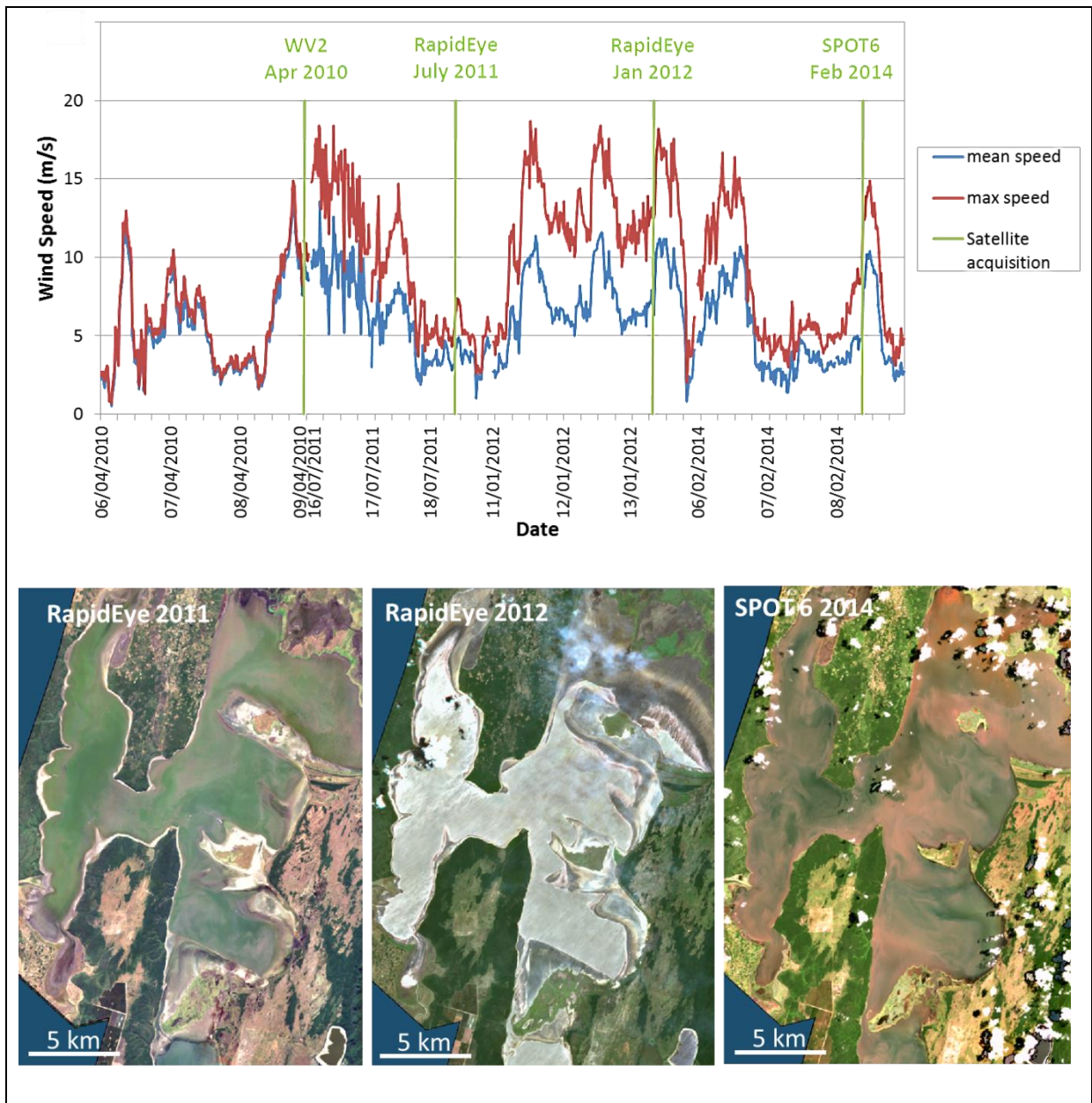
Overall Classification Accuracy = 57.83%

Overall Kappa Statistics = 0.51

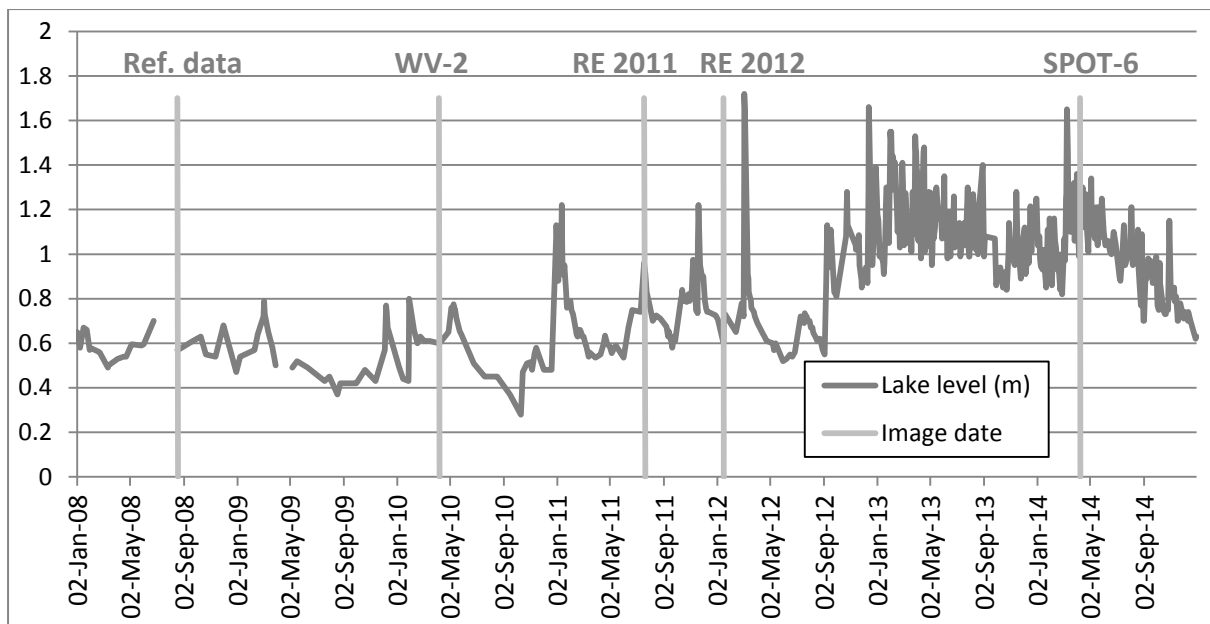
463
 464 Striking however is the high degree of confusion and misclassification of the Bare Soil and
 465 Water classes in both, the 2011 and the 2012 RapidEye images. In most land cover or
 466 vegetation classifications these classes usually produce accuracies of 75%, 80% or better.
 467 Figure 5 and Figure 6 might explain the results. At the bottom of Figure 5 subsets of the
 468 Lakes area of the RapidEye and SPOT-6 images are displayed in natural (true) colour. The
 469 WorldView-2 image unfortunately did not cover this area. The estuary's water body looks
 470 very different in all three images. In the July 2011 image, the water level appears to be
 471 moderately high, in the January 2012 image the water level is very low, and in the 2014
 472 SPOT-6 image the water level appears to be very high. These observations are supported by
 473 the measured water levels at the St Lucia Bridge (Figure 6). The water level at the time of
 474 acquisition of the 2010 WV-2 image is about the same at the reference time in 2008. The
 475 comparable hydrologic conditions with no major water level changes between the two dates
 476 resulted in vegetation similarity and contributed to the high accuracies of the WV-2
 477 classification.

478

479



480 **Figure 5: Top: Hourly wind speed, measured at Richardsbay for 2011-2014 and Durban**
 481 **for 2010 (no Richardsbay data available for 2010), for three days prior to respective**
 482 **satellite image acquisition dates. Bottom: Subset of respective RapidEye and SPOT-6**
 483 **images for the North Lake and False Bay area of the estuary. Wind data source:**
 484 **SADCO (<http://sadco.csir.co.za/>).**
 485



486

487 **Figure 6: Water level at the St Lucia Estuary, measured at the St Lucia Bridge (source:**
 488 **Ezemvelo KZN Wildlife). Grey bars: 4x image acquisition dates and 2008 date of**
 489 **reference data collection.**

490

491 The difference in the 2011 and 2012 water levels and the peak water levels in between the
 492 reference and image acquisition dates might explain the confusion of the classes which are to
 493 be found close to the water edge, as their position will probably have been different from the
 494 reference GIS map or vegetation mapped in 2008 might have been washed away during the
 495 floods. This result is supported by Rautenbach (2015) who noted: *“The biggest change in*
 496 *vegetation composition [between 2008 and 2013] was the overall decrease in salt marsh (by*
 497 *57%) and increase in submerged macrophytes (by 96%). After the drought [in 2010], water*
 498 *level rose rapidly as rainfall returned to normal and the Mfolozi River connected to the sea*
 499 *and St Lucia Estuary. This caused an increase in surface area of the water column (which*
 500 *includes the Lakes, Narrows, Back Channel, Link Canal and Mfolozi River) from 30 498 ha*
 501 *in 2008 to 32 624 ha in 2013. The increase in water level and the reduction in salinity in*
 502 *False Bay and the lakes (North and South) caused flooding and inundation of the salt marsh*
 503 *habitat, reducing the area covered.”*

504 The colour of the water at the image acquisition dates is another potential source for
505 misclassification. In the SPOT-6 image the water looks relatively clear with only a slight
506 brown discolouration indicating some small degree of turbidity. This maybe a result of the
507 mixing of the strong winds two days before the image was taken (Figure 5, top). Given the
508 high water levels at that time, the mixing of the water column would only have been
509 moderate. Flow from the Mfolozi River and entry of water via the back channel and link
510 canal would also result in increased turbidity particularly in the Narrows.

511 In the 2011 image however, the water looks greenish, indicating some degree of chlorophyll,
512 either from some microalgae bloom or by submerged macrophyte development. This
513 observation was confirmed by Taylor et al. (2013) who reported high coverages of
514 macrophyte beds in that area which vanished after May 2013. The misclassification of Water
515 as Bare soil (Table 6) supports this observation when considering that our Bare soil based on
516 an NDVI <0.4 likely included some vegetation signal.

517 In the 2012 RapidEye image, the water looks very turbid and turbulent. Figure 5 and Figure 6
518 show that the water level at that time was very low and that during the three days preceding
519 the image capture a strong (south-easterly) wind was blowing. Under these conditions the
520 water column would have been mixed up and very turbid and the water surface very rough
521 with wind generated waves. (The waves are actually visible when zooming into the image.)
522 This explains the high degree of misclassification between bare soil and water in this image.

523

524 **5. Conclusions**

525 This paper examined the value of very high resolution multispectral satellite imagery from
526 the WorldView-2 (2 m pixel size), RapidEye (5m pixel size) and SPOT-6 (5m pixel size)
527 sensors acquired between 2010 and 2014 and LiDAR derived digital surface information for
528 classifying estuarine vegetation types. Ground truthing reference was a GIS-based vegetation

529 map from 2008. Supervised maximum likelihood classification produced satisfactory overall
530 accuracies for the WorldView-2 and the SPOT-6 image, while the RapidEye-based
531 classifications produced slightly lower overall accuracies.

532 However, the analysis of classification errors in relation to environmental factors showed that
533 mainly high vegetation dynamics, adverse wind conditions, different water levels and
534 resulting water turbidity seem to be the reason for the observed misclassifications rather than
535 weaknesses of the imagery itself.

536 It is the inherent dynamic nature of the estuarine environment with large fluctuations in water
537 levels and salinity, which causes swift turn-over of vegetation types, temporally and spatially.
538 Examples include Salt marsh to Sedges and Reeds, or Grass and Shrubs to Swamp forest on
539 abandoned Forest plantations. This leads to inaccurate vegetation classifications if the
540 acquisition date of satellite imagery and the validation data are too far apart. In the St Lucia
541 Estuary, even 6-12 months difference turned out to lead to major vegetation change and
542 hence misclassification, if a major flood eradicated entire vegetation patches or even a recent
543 wind event occurred. It is therefore recommended that ground truthing data are to be used
544 that match the satellite image acquisition dates as closely as possible.

545 Results were also influenced by physiognomic and spectral similarity of certain vegetation
546 types, such as grass and reeds, and shrubs and forests. This confusion is technically expected.
547 The additional use of LiDAR-derived Digital Surface Models improved the separability of
548 those classes and improved 5 out of 8 classification runs. Further solutions could include
549 either the use of a sensor with a better (hyperspectral) resolution of the satellite imagery or
550 possibly by a more conscious choice of the image acquisition date, where spectral
551 separability varies over the seasons.

552 Apart from true vegetation change, recent weather impacts (high water levels inundating
553 terrestrial vegetation and wind events mixing up the water column) also contribute to a bias

554 in the reflective properties of the satellite imagery and impair the accurate identification of
555 surface and vegetation types.

556 Our research showed the importance of ancillary environmental condition data such as water
557 levels, mouth state, wind and weather data to interpret results appropriately. For dynamic
558 environments, such as estuaries and the coast, these data should be sourced routinely as part
559 of any remote sensing based vegetation assessment study. This is even more important under
560 (so frequently experienced) project conditions where ground truthing data of the same period
561 are not available.

562 This research also shows that remote sensing may potentially be more successfully applied to
563 the large permanently open estuaries (~ 30 of South Africa's systems) as their habitats are
564 more stable than the systems that close with large fluctuations in water levels.

565 The results show that the spatial and spectral resolution of modern very high resolution
566 imagery is sufficient to satisfactory map and monitor small scale estuarine vegetation. They
567 emphasize however the importance of synchronisation of ground truthing data with actual
568 image acquisition times in these highly dynamic environments.

569

570 **6. Acknowledgements**

571 The authors gratefully acknowledge the various sources of funding that enabled the presented
572 research, namely the GEF (Global Environmental Facility) Project via iSimangaliso Wetland
573 Park Authority for funding Kelly Rautenbach's MSc thesis at the Nelson Mandela
574 Metropolitan University; the Water Research Commission through the research project WRC
575 K5/2268 "Understanding estuarine processes in UMfolozi/Msundazi/St Lucia estuary from
576 earth observation data of vegetation composition, distribution and health" and a
577 Parliamentary Grant to the CSIR's Coastal Systems Research Group for closing loops and
578 writing up. Further to the iSimangaliso Wetland Park for access for field visits, invaluable

579 discussions and access to the LiDAR data of the area that were acquired for its GEF project
580 “Development, Empowerment and Conservation in the iSimangaliso Wetland Park and
581 Surrounding Region Project”. Satellite imagery has been provided by the BlackBridge
582 Company (RapidEye), EADS through the South African National Space Agency (SPOT-6)
583 and DigitalGlobe (WorldView-2).

584

585 **7. References**

586 Adam, E., Mutanga, O., 2009. Spectral discrimination of *papyrus* vegetation (*Cyperus papyrus* L.) in
587 swamp wetlands using field spectrometry. ISPRS Journal of Photogrammetry and Remote Sensing 64,
588 612-620.

589 Adam, E., Mutanga, O., Odindi, J., Abdel-Rahman, E. M., 2014. Land-use/cover classification in a
590 heterogeneous coastal landscape using RapidEye imagery: evaluating the performance of random
591 forest and support vector machines classifiers. International Journal of Remote Sensing 35 (10), 3440-
592 3458.

593 Cowan, G. I., 1999. The St Lucia System. Available online at: [<http://hdl.handle.net/1834/460>]. Last
594 accessed 17 Nov. 2015.

595 Dogan, O. K., Akyurek, Z., Beklioglu, M., 2009. Identification and mapping of submerged plants in a
596 shallow lake using Quickbird satellite data. Journal of Environmental Management 90, 2138-2143.

597 Duro, D. C., Franklin, S. E., Dubé, M. G., 2012. A Comparison of Pixel-Based and Object-Based
598 Image Analysis with Selected Machine Learning Algorithms for the Classification of Agricultural
599 Landscapes Using SPOT-5 HRG Imagery. Remote Sensing of Environment 118, 259-272.

600 EPA, 2013. <http://water.epa.gov/scitech/swguidance/standards/criteria/aqlife/biocriteria/index.cfm>.
601 Last accessed 17 Nov. 2015.

602 Fyfe, S. K., 2003. Spatial and temporal variation in spectral reflectance: are seagrasses spectrally
603 distinct? Limnology & Oceanography 48, 464-479.

604 GTI, 2010. 2008 KZN Province Land-Cover Mapping (from SPOT 5 Satellite imagery ca. 2008) –
605 Data Users Report and Meta Data (version 1.0). Published by GeoTerraImage GTI (Pty) Ltd, South
606 Africa, for Ezemvelo KZN Wildlife (Biodiversity Research). October 2010.

607 Harvey, K.R., Hill, J.E., 2001. Vegetation mapping of a tropical freshwater swamp in the Northern
608 Territory, Australia: a comparison of aerial photography, Landsat TM and SPOT satellite imagery.
609 *Remote Sensing of Environment* 22, 2911-2925.

610 Kempeneers, P., Deronde, B., Provoost, S., Houthuys, R., 2009. Synergy of Airborne Digital Camera
611 and Lidar Data to Map Coastal Dune Vegetation. *Journal of Coastal Research* 53, 73-82.

612 Lillesand, T. M., Kiefer, R.W., Chipman, J.W., 2004. *Remote Sensing and Image Interpretation*. Fifth
613 Edition. John Wiley & Sons, New York.

614 Loveland, T.R., Merchant, J.W., Ohlen, D.O., Brown, J.F., 1991. Development of a Land-Cover
615 Characteristics Database for the Conterminous U.S.. *Photogrammetric Engineering & Remote*
616 *Sensing* 57 (11), 1453-1463.

617 Lowry, J., Ramsey, R.D., Thomas, K., Schrupp, D., Sajwaj, T., Kirby, J., Waller, E., Schrader, S.
618 Falzarano, S., Langs, L., Manis, G., Wallace, C., Schulz, K., Comer, P., Pohs, K., Rieth, W.,
619 Velasquez, C., Wolk, B., Kepner, W. Boykin, K., O'Brien, L., Bradford, D., Thompson, B., Prior-
620 Magee, J., 2007. Mapping Moderate-Scale Land-Cover over Very Large Geographic Areas within a
621 Collaborative Framework: A Case Study of the Southwest Regional Gap Analysis Project
622 (SWReGAP). *Remote Sensing of Environment* 108 (1), 59-73.

623 Lunetta, R.S., Knight, J.F., Ediriwickrema, J., Lyon, J.G., Worthy, L.D., 2006. Land-cover change
624 detection using multi-temporal MODIS NDVI data, *Remote Sensing of Environment* 105 (2), 142-
625 154.

626 Moll, E.J., Ward, C.J., Steinke, T.D., Cooper, K.H., 1971. Our mangroves threatened. *African*
627 *Wildlife* 26, 103-107.

628 Nondoda, S. P., 2012. *Macrophyte distribution and responses to drought in the St. Lucia Estuary*.
629 MSc. thesis, Nelson Mandela Metropolitan University (NMMU), South Africa.

630 Prisloe, S., Wilson, M., Civco, D., Hurd, J., Gilmore, M., 2006. Use of Lidar data to aid in
631 discriminating and mapping plant communities in tidal marshes of the lower Connecticut River:

632 preliminary results. In: Annual Conference of the American Society for Photogrammetry and Remote
633 Sensing. Presented at the Prospecting for Geospatial Information Integration. American Society for
634 Photogrammetry and Remote Sensing, Nevada.
635 <ftp://jetty.ecn.purdue.edu/jshan/proceedings/asprs2006/files/0119.pdf>, Last accessed 17 Nov. 2015.
636 Rautenbach K, 2015. Present state of Macrophytes and responses to management scenarios at the St.
637 Lucia and Mfolozi estuaries. MSc thesis, Nelson Mandela Metropolitan University (NMMU), South
638 Africa.
639 Schuster, C., Förster, M., Kleinschmit, B., 2012. Testing the Red Edge Channel for Improving Land-
640 Use Classifications Based on High-Resolution Multi-Spectral Satellite Data. International Journal of
641 Remote Sensing 33 (17), 5583-5599.
642 Silva, T.S.F., Costa, M.P.F., Melack, J.M., Novo, E., 2008. Remote sensing of aquatic vegetation:
643 theory and applications. Environmental Monitoring and Assessment 140, 131-145.
644 Taylor, R. H., 2006. Ecological responses to changes in the physical environment of the St. Lucia
645 Estuary. PhD Thesis, Norwegian University of Life Sciences. Papers 1, 2 and 3.
646 Taylor, R., Adams, J.B., Haldorsen, S., 2006. Primary Habitats of the St Lucia Estuarine System,
647 South Africa, and their Responses to Mouth Management. African Journal of Aquatic Science 31 (1),
648 31-41.
649 Taylor, R., Fox, C., Mfeka, S., 2013. Monitoring the St Lucia Estuarine System: A synthesis and
650 interpretation of the monitoring data for May 2013. Unpublished Ezemvelo KZN Wildlife report. 16
651 pages.
652 Townshend, J. R. G., Justice, C.O., Gurney, C., McManus, J., 1992. The Impact of Misregistration on
653 Change Detection. IEEE Transactions on Geoscience and Remote Sensing 30(5), 1054-1060.
654 Turpie, J.K., Wilson, G., Van Niekerk, L., 2012. National Biodiversity Assessment 2011: National
655 Estuary Biodiversity Plan for South Africa – Technical Report. Anchor Environmental Consultants
656 Report No. AEC2012/01, Cape Town.
657 UNESCO 1999. UNESCO World Heritage Committee, Report of the 23rd Session, Marrakesh,
658 Morocco, 29 Nov- 4 Dec 1999. WHC Report No. WHC-99/CONNF.209/22, Paris, March 2000.

659 Available online at <http://whc.unesco.org/archive/1999/whc-99-conf209-22e.pdf>. Last accessed 17
660 Nov. 2015.

661 Van Heerden, I. L., 2011. Management concepts for the Mfolozi flats and estuary as a component of
662 the management of the iSimangaliso Wetland Park. In: Bate, G.C., Whitfield, A.K., Forbes, A.T.
663 (Eds.) 2011. A review of studies on the Mfolozi estuary and associated flood plain, with emphasis on
664 information required by management for future reconnection of the river to the St Lucia system.
665 Report to the Water Research Commission. WRC Report No. KV 255/10. Pretoria: WRC.

666 Van Niekerk, L., Turpie, J.K. (eds) 2012. South African National Biodiversity Assessment 2011:
667 Technical Report. Volume 3: Estuary Component. CSIR Report Number CSIR/NRE/ECOS/ER/2011
668 /0045/B. Council for Scientific and Industrial Research, Stellenbosch.

669 Whitfield, A. K., 1992. A characterization of Southern African Estuarine Systems. South African
670 Journal of Aquatic Science 18, 89-103.

671 Yang, X., 2007. Integrated use of remote sensing and geographic information systems in riparian
672 vegetation delineation and mapping. International Journal of Remote Sensing 28, 353-370.